A retained intron in the 3′-UTR of *Calm3* mRNA mediates its Staufen2- and activity-dependent localization to neuronal dendrites

Tejaswini Sharangdhar[1], Yoichiro Sugimoto[2,3], Jacqueline Heraud-Farlow[4,†], Sandra M Fernández-Moya[1], Janina Ehses[1], Igor Ruiz de los Mozos[2,3] (iD), Jernej Ule[2,3] (iD) & Michael A Kiebler[1,*] (iD)

Abstract

Dendritic localization and hence local mRNA translation contributes to synaptic plasticity in neurons. Staufen2 (Stau2) is a well-known neuronal double-stranded RNA-binding protein (dsRBP) that has been implicated in dendritic mRNA localization. The specificity of Stau2 binding to its target mRNAs remains elusive. Using individual-nucleotide resolution CLIP (iCLIP), we identified significantly enriched Stau2 binding to the 3′-UTRs of 356 transcripts. In 28 (7.9%) of those, binding occurred to a retained intron in their 3′-UTR. The strongest bound 3′-UTR intron was present in the longest isoform of *Calmodulin 3* (*Calm3$_L$*) mRNA. *Calm3$_L$* 3′-UTR contains six Stau2 crosslink clusters, four of which are in this retained 3′-UTR intron. The *Calm3$_L$* mRNA localized to neuronal dendrites, while lack of the 3′-UTR intron impaired its dendritic localization. Importantly, Stau2 mediates this dendritic localization via the 3′-UTR intron, without affecting its stability. Also, NMDA-mediated synaptic activity specifically promoted the dendritic mRNA localization of the *Calm3$_L$* isoform, while inhibition of synaptic activity reduced it substantially. Together, our results identify the retained intron as a critical element in recruiting Stau2, which then allows for the localization of *Calm3$_L$* mRNA to distal dendrites.

Introduction

Dendritic mRNA localization enables neurons to alter the synaptic proteome thereby inducing plastic changes at selected synapses [1]. In this multi-step process, a selected set of RNA-binding proteins (RBPs) assembles mRNAs containing *cis*-acting sorting signals into ribonucleoprotein particles (RNPs) that are then transported along the cytoskeleton into dendrites, near synapses [2]. Specific regulation of local mRNA translation at synapses in response to synaptic stimuli then allows long-term synaptic plasticity, the cellular basis for learning and memory. Moreover, several other aspects of mRNA regulation, from nuclear RNA splicing to mRNA stability, play crucial roles in the adaptation of the synaptic proteome that is required to maintain synaptic homeostasis [3]. Several studies have recently reported extensive alternative splicing in neurons [4]. Furthermore, alternative polyadenylation in neurons leads to a variety of mRNA isoforms of the same transcript differing only in their 3′-UTR length [5]. Together, these phenomena give rise to mRNAs, all expressing the same polypeptide, but harboring additional regulatory elements that recruit the neuronal RBPs necessary for fine post-transcriptional regulation [3,4].

Staufen2 (Stau2) is a well-known neuronal double-stranded RBP (dsRBP) involved in asymmetric cell division of neural progenitor cells and has been implicated in dendritic RNA localization, in mature hippocampal neurons [6–9]. Previously, we identified a repertoire of physiologically relevant target mRNAs from neuronal Stau2-containing RNA granules [10]. For some of these targets (e.g., *Rgs4*, *Cplx1*), Stau2 influences their mRNA stability. However, only 38 of the 1,169 Stau2 targets identified by Stau2 IP (3.2%) show changes in mRNA levels upon Stau2 downregulation [10]. Thus, Stau2 function is not restricted to regulation of mRNA stability.

It is unclear how Staufen proteins bind to their target mRNAs with the observed specificity, with several studies coming to different conclusions [11,12], and even some studies suggesting its binding to be non-sequence-specific [8]. Hence, we applied individual-nucleotide resolution CLIP (iCLIP) [13] as this yields information about the direct Stau2 binding to its mRNA targets with higher resolution compared to Stau2 IP microarray experiments previously performed [10]. This approach allowed us to uncover significant

1   Division of Cell Biology, Biomedical Center, LMU Munich, Martinsried, Germany
2   Department of Molecular Neuroscience, University College London Institute of Neurology, London, UK
3   The Francis Crick Institute, London, UK
4   DK RNA Biology, M.F. Perutz Laboratories, Vienna, Austria
   *Corresponding author. Tel: +49 89 2180 75 884; E-mail: mkiebler@lmu.de
   †Present address: St Vincent's Institute of Medical Research, Fitzroy, Vic., Australia

Stau2 binding to 3′-UTRs of 356 mRNAs, and 28 of these retained an intron in their 3′-UTR. The strongest Stau2 binding within a retained intron was seen in the 3′-UTR of the longest isoform of *Calmodulin 3* (*Calm3$_L$*) transcript. Interestingly, *Calm3$_L$* is the top target identified by both iCLIP and Stau2 IP microarray. Furthermore, we showed that *Calm3$_L$* mRNA localized to dendrites in hippocampal neurons and that NMDA-mediated neuronal activation specifically promoted dendritic localization of the intron-containing *Calm3$_L$* mRNA. Importantly, neither neuronal activation/silencing nor Stau2 knockdown showed any changes in total *Calm3* mRNA levels. We then set out to investigate a direct role of Stau2 in dendritic mRNA localization of *Calm3$_L$*. Finally, we demonstrated that the recruitment of Stau2 to the *Calm3$_L$* mRNA allows its dendritic localization.

Results and Discussion

iCLIP reveals specific binding of Stau2 to *Calm3* mRNA via a retained intron

In order to get a mechanistic insight into Stau2 binding to mRNAs, we performed iCLIP experiments. We immunoprecipitated the endogenous Stau2-RNA complexes from embryonic day 18 (E18) mouse brains by using an antibody against Stau2 (Dataset EV1). IPs using a rabbit pre-immune serum (PIS) were done in parallel as negative control. We compared our results with the iCLIP data of other two RBPs (TDP-43 and FUS) that were also produced from E18 mouse brains [14]. Here, we identified significant Stau2 binding in 3′-UTRs of 356 neuronal mRNAs (Table EV1). For 28 of these, the binding sites in 3′-UTRs were found in the retained introns (Fig 1A; Table EV2). Figure EV1A shows three examples of such mRNAs with Stau2 binding sites within a retained 3′-UTR intron. Among these, *Calm3* mRNA stood out as the top Stau2 mRNA target with a retained 3′-UTR intron and with 0.24% of all iCLIP tags on mRNAs originating from *Calm3*. This binding was specific for *Calm3* transcripts, but not the other calmodulin orthologs (*Calm1*, *Calm2*) [15], that do not contain any crosslink clusters. This was confirmed by IP experiments: Only *Calm3* transcripts were highly enriched in the immunoprecipitates of Stau2-containing RNPs (Fig 1B) [10], but no enrichment was obtained with control PIS IPs. In rat brain, three mRNA isoforms of *Calm3* have been reported, which differ in their 3′-UTR length [15]. In primary rat cortical neurons, we only observed the presence of two isoforms (Fig EV1B), the longest of which (*Calm3$_L$*) contains a retained intron in its 3′-UTR. Our iCLIP analysis revealed that the *Calm3* mRNA contains six high-confidence crosslink clusters in the 3′-UTR of the *Calm3$_L$* isoform, four of which overlapped with the retained intron (Fig 1C, upper panel). The lower panel in Fig 1C shows the specific positions of these Stau2 crosslink clusters on a predicted structure of the *Calm3$_L$* 3′-UTR. These positions were located right next to the long-range predicted RNA duplexes. The cluster with most crosslinking (cluster 2) was located next to a predicted long-range duplex, which bridged regions of 3′-UTR that are ± 700 nt apart. This observation is in agreement with the previous finding that long-range duplexes in 3′-UTRs of mRNAs are enriched on Stau1 binding sites [16]. Importantly, no high-confidence crosslink clusters were detected in other intronic regions of *Calm3* transcript (data not shown).

The expression of *Calm3$_L$* isoform increased with the development of *in vitro*-cultured hippocampal (Figs 1G and EV1D) and rat cortical neurons (RCN) (Figs 1H and EV1C) and reached maximal levels in mature neurons that have undergone synaptogenesis (stage 5 neurons; see [17]). *Calm3$_L$* mRNA localizes mainly in the somato-dendritic compartment. Also, its localization was restricted to the MAP2-positive neuronal processes (i.e., dendrites) but not to the MAP2-negative ones (Fig 1D and F). Importantly, Stau2 co-localized with the *Calm3$_L$* mRNA endogenously (Fig 1E).

Synaptic activity regulates *Calm3* mRNA localization via the retained 3′-UTR intron in hippocampal neurons

Localization of an mRNA to dendrites can lead to its local translation and hence spatio-temporal regulation of its function. This localization is known to be influenced by neuronal activity [18]. Therefore, we analyzed the effect of neuronal activation and

Figure 1. The intron-containing *Calm3* mRNA isoform interacts with Stau2 and localizes to dendrites.

A   The proportion of cDNAs (out of all cDNAs that mapped to the mouse genome) produced by iCLIP (using E18 mouse brain extracts) from the FUS, TDP-43, and Stau2 experiments that mapped to different RNA regions (i.e., UTR: untranslated region; CDS: coding sequence) and intergenic regions (i.e., non-annotated transcripts).

B   Relative values of *Calm3, Calm2,* and *Calm1* mRNA enrichment upon control or anti-Stau2 IPs from E17.5 rat brains. Pre-immune serum was used to perform control IPs; n = 3, average + SEM.

C   iCLIP results show that Stau2 specifically binds to the longest *Calm3* (*Calm3$_L$*) isoform retaining an intron in its 3′-UTR (schematic in the middle). Lower panel shows the specific positions of these Stau2 crosslink clusters on a predicted structure of the *Calm3$_L$* mRNA.

D   Representative images of endogenous *Calm3$_L$* mRNA in rat primary hippocampal neurons (DIV15) visualized by a FISH probe directed against the intron (*Calm3* intron FISH; red). Magnified insets (40-μm dendritic sections) below identify MAP2-positive (box 1; MAP2 in green) and MAP2-negative (box 2) neuronal processes; arrowheads indicate the FISH signal for *Calm3$_L$* in the dendritic section; nucleus (DAPI; blue). Boxes on the top right show images of bright field (above) and (below) Stau2 (purple) co-staining with DAPI (cyan); asterisk denotes the soma of the neuron under study; scale bar, 20 μm.

E   Co-localization of endogenous Stau2 with endogenous *Calm3$_L$* mRNA in the panel represented in (D). Arrowheads indicate dendritic co-clusters (*Calm3* intron FISH; green) and Stau2 immunostaining (purple); inset (top right) shows Stau2 staining in the soma at low exposure. The white perforated line marks the position of the nucleus; scale bar, 20 μm.

F   Quantification of the number of spots of *Calm3$_L$* mRNA per length (40-μm region) in MAP2-positive and MAP2-negative neuronal processes; average + SEM taken from three independent experiments (30 dendrites each), ***P < 0.001, unpaired Mann–Whitney U-test.

G   Quantification of the cell body intensity normalized to area to measure levels of *Calm3$_L$* mRNA in different stages of *in vitro* development of rat hippocampal neurons (1, 4, 8, 12, and 15 DIV), n = 3, average + SEM, t-test; *P < 0.05, **P < 0.01.

H   qRT–PCR experiments to measure the relative levels of *Calm3$_L$* to total *Calm3* mRNA in E17.5 or adult rat cortex and 0, 2, 4, and 6–7 DIV rat cortical neurons; n = 3, average + SEM, t-test; *P < 0.05, **P < 0.01, ***P < 0.001.
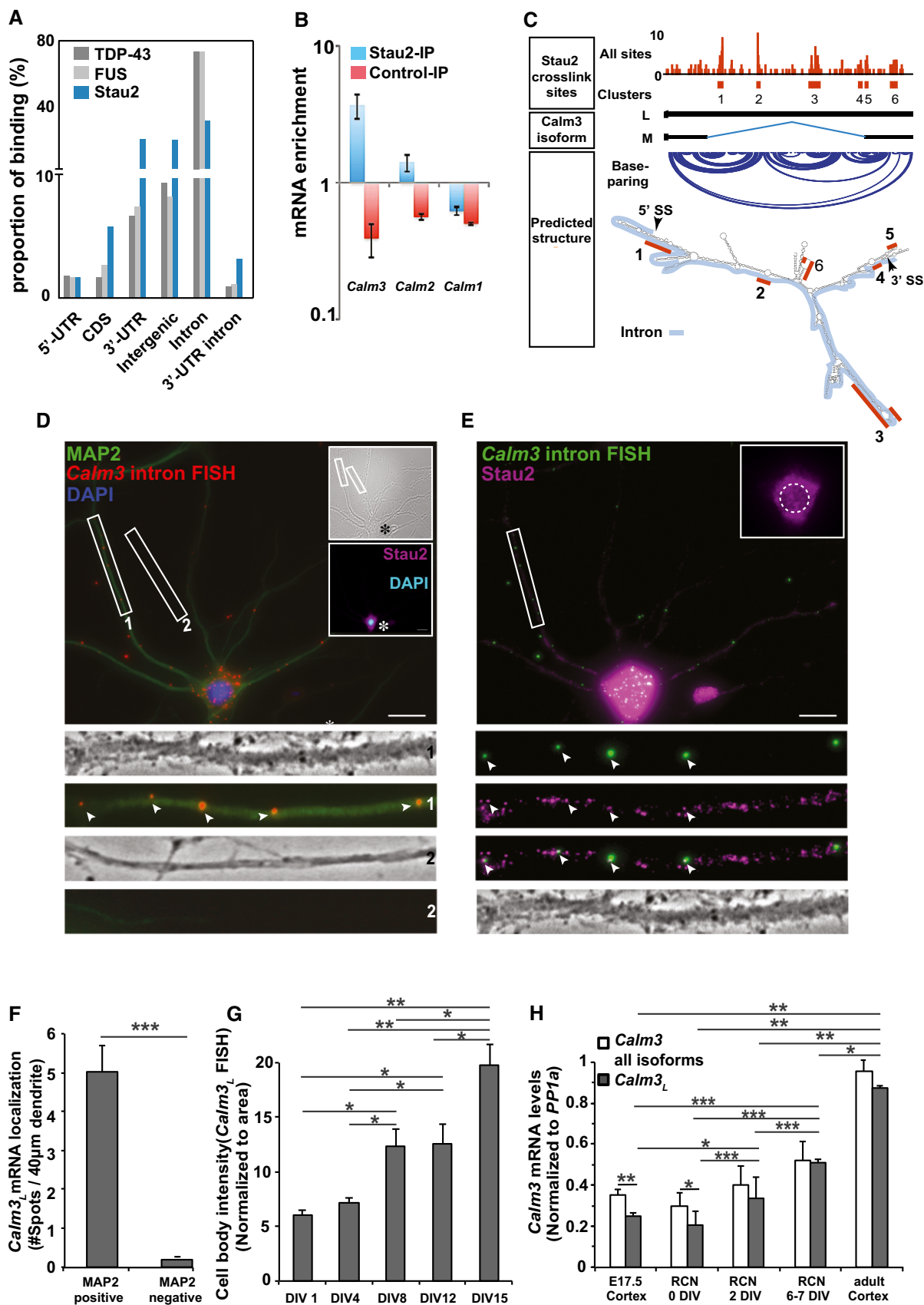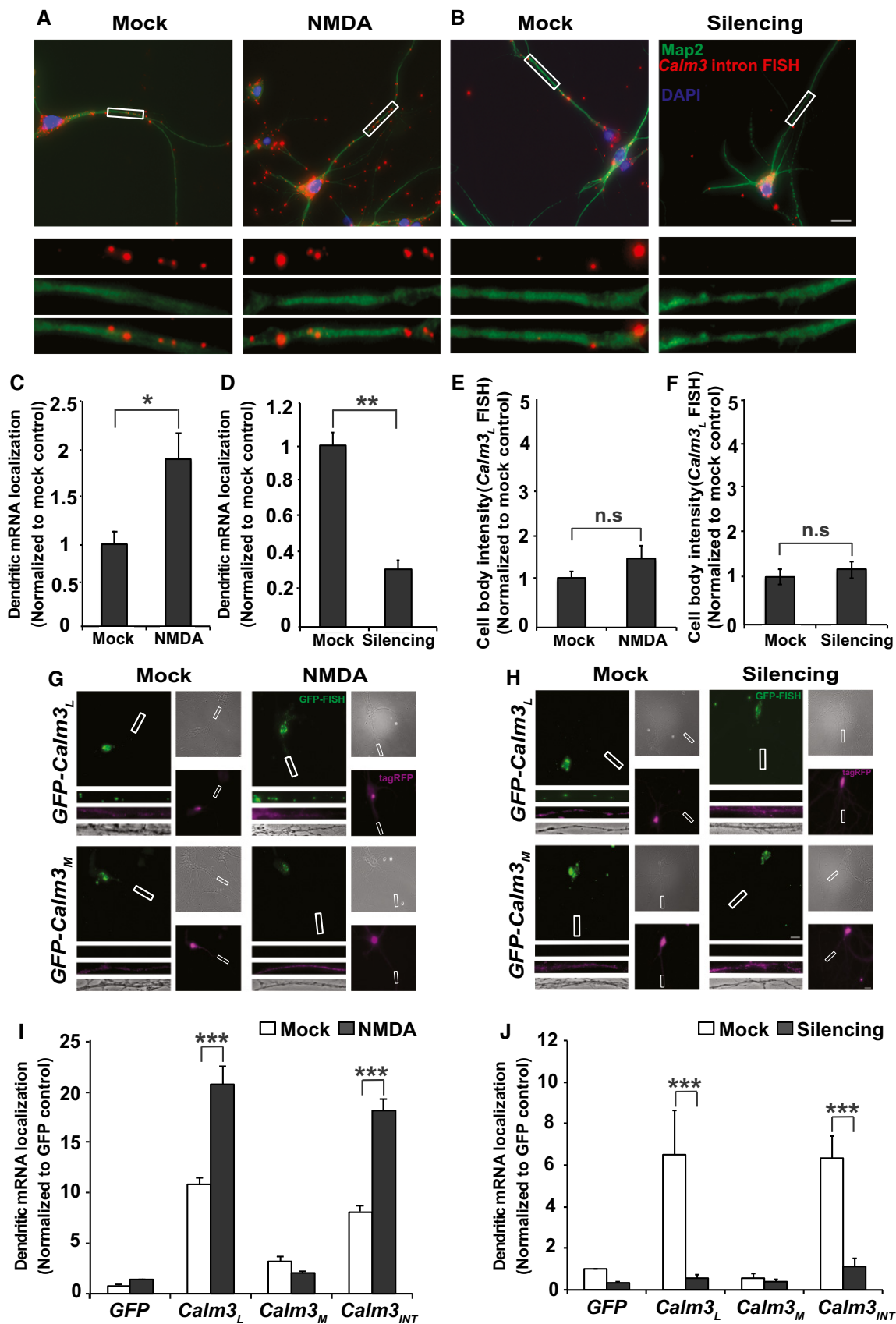
Figure 1.

Figure 2.

Figure 2. Neuronal activity regulates dendritic localization of *Calm3* intron-containing endogenous and *GFP* reporter RNAs.

A, B   Representative *Calm3* intron FISH images of primary rat hippocampal neurons (DIV12) that were either stimulated by NMDA (15 min) (A) or silenced O/N (B) using a standard cocktail containing TTX, CNQX, and AP5 (see Materials and Methods). Mock-treated neurons serve as the respective controls. Dendrites are visualized with anti-MAP2 staining (green) and nuclei with DAPI (blue). Insets below show 40-μm dendritic sections marked by white boxes. Scale bar, 20 μm.

C, D   Quantification of dendritic localization experiments shown in panels (A) and (B), respectively. Bars represent the mean number of spots per 40-μm dendritic section normalized to control + SEM taken from three independent experiments. Selected dendritic regions were at least 2 cell body diameters away from the soma. $n \geq 30$ dendrites per condition; *$P < 0.05$; **$P < 0.01$; unpaired Mann–Whitney U-test.

E, F   Quantification of fluorescence intensity in the cell body for $Calm3_L$ mRNA (detected by *Calm3* intron FISH) upon neuronal stimulation by NMDA (15 min) (E) or silencing O/N (F) of three different experiments as shown in panels (A) and (B), respectively. Values are normalized to respective controls; $n = 3$; mean number of spots per 40-μm dendritic section normalized to control + SEM, t-test, $P > 0.05$, n.s. = not significant.

G, H   Representative images of primary rat hippocampal neurons (DIV11) expressing TagRFP (purple) together with either GFP-$Calm3_L$ (upper rows) or GFP-$Calm3_M$ (lower rows) that were stimulated by NMDA (15 min) (G) or silenced O/N (H) using a standard cocktail containing TTX, CNQX, and AP5 (the same as in panels A and B; see Materials and Methods). Bright-field images are also included. Mock-treated neurons serve as the respective controls. *GFP* mRNA is detected using a GFP FISH probe. Insets below each image show 40-μm dendritic sections marked by white boxes. Scale bar, 20 μm.

I, J   Quantification of dendritic localization in panels (G) and (H). Bars represent the mean number of spots per 40-μm dendritic section normalized to control + SEM taken from three independent experiments. Selected dendritic regions were at least 2 cell body diameters away from the soma. $n \geq 30$ dendrites per condition; ***$P < 0.001$; unpaired Mann–Whitney U-test.

silencing on the observed dendritic localization of endogenous $Calm3_L$ in rat hippocampal neurons (DIV12). The dendritic localization of $Calm3_L$ mRNA increased upon NMDA treatment (Fig 2A and C), and it decreased drastically upon neuronal silencing (Fig 2B and D) (see Materials and Methods). Importantly, these treatments did not affect total $Calm3_L$ mRNA levels as fluorescence *in situ* hybridization (FISH) signal intensity in the cell body (Fig 2E and F) and qPCR values (Fig EV2D) were not modified. Next, we investigated in detail the role of the 3′-UTR intron in the dendritic localization of *Calm3* transcripts. As the endogenous short isoform of *Calm3* ($Calm3_M$; lacking the retained exon) cannot be identified specifically due to overlapping sequences with the $Calm3_L$, we took advantage of a *GFP* mRNA reporter assay. We generated several GFP reporters, which contained different *Calm3* 3′-UTRs (scheme in Fig EV2E). We analyzed the localization of the *GFP* reporters in rat hippocampal neurons upon NMDA stimulation or synaptic silencing by FISH against the *GFP* sequence. The dendritic localization of *GFP* transcripts containing the intron ($Calm3_L$ and $Calm3_{INT}$) increased upon neuronal stimulation (Figs 2G and I, and EV2A) and was dramatically reduced upon synaptic silencing (Figs 2H and J, and EV2B). These data showed that the *Calm3* intron in the 3′-UTR is sufficient to confer activity-dependent changes in *GFP* mRNA localization. Moreover, neither of these

pharmacological treatments altered the total *GFP* mRNA levels in $Calm3_L$ and $Calm3_{INT}$ reporters (Fig EV2C). Together, these experiments showed that neuronal activity regulated dendritic localization of $Calm3_L$ mRNA via the 3′-UTR intron without altering its total levels.

Staufen2-mediated dendritic localization of *Calm3* mRNA via its 3′-UTR intron

To investigate whether Stau2 directly mediates dendritic localization of intron-containing transcripts, we evaluated the subcellular localization of the different GFP mRNA reporters when they were co-expressed with the exogenous 62-kDa isoform of Stau2 (TagRFP-Stau2[62]). TagRFP-Stau2[62] expression significantly increased the dendritic localization of the intron-containing reporter mRNAs (Figs 3A and B, and EV3A and B). The presence of the intron in the reporter constructs ($Calm3_L$ and $Calm3_{INT}$) was confirmed by qPCR (Fig 3H). Importantly, exogenous TagRFP-Stau2[62] expression did not alter the mRNA levels of either $Calm3_L$ and $Calm3_{INT}$ GFP or luciferase reporter constructs (Fig EV3C and D) or endogenous $Calm3_L$ mRNA (Fig 3F and G). This highlighted the dependence of *Calm3* mRNA on the *cis*-element (i.e., the *Calm3* intron) and the *trans*-factor (i.e., Stau2) for its localization. Moreover, the

Figure 3. Stau2 overexpression increases the dendritic localization of *Calm3* intron-containing GFP reporter mRNA.

A   Representative images of primary rat hippocampal neurons (DIV12) co-expressing either GFP-$Calm3_L$ (upper rows) or GFP-$Calm3_M$ (lower rows) together with either TagRFP (left) or TagRFP-Stau2[62] (both in purple) (right). *GFP* mRNA is detected using a GFP FISH probe (green). Bright-field images are also shown. Arrowheads in the top right panel indicate co-localization. Insets below each image show 40-μm dendritic sections marked by white boxes. Scale bar, 20 μm.

B   Quantification of dendritic localization of the different GFP reporters identified by GFP FISH upon co-transfection together with either TagRFP or TagRFP-Stau2[62] as shown in (A). Bars represent the mean number of spots per 40-μm dendritic section normalized to control + SEM taken from three independent experiments. $n \geq 30$ dendrites per condition. **$P < 0.01$, ***$P < 0.001$, unpaired Mann–Whitney U-test.

C, D   Representative images of neurons co-transfected with the GFP-$Calm3_{INT}$ reporter (mRNA identified by GFP FISH) together with either the RBP TagRFP-Stau2[62] (C) or the unrelated RBP TagRFP-Pum2 (D). Bright-field images are also shown. Insets below each image show 100-μm dendritic sections marked by white boxes in the main image. Arrowheads indicate dendritic co-clusters. Scale bar, 20 μm.

E   Quantification of the percentage of co-localization of GFP-$Calm3_{INT}$ total GFP mRNA spots together with TagRFP-Stau2 or TagRFP-Pum2 within a 100-μm dendritic section as shown in panels (C) and (D); mean + SEM, taken from three independent experiments. $n \geq 40$ dendrites per condition. Selected dendritic regions were at least 2 cell body diameters away from the soma. ***$P < 0.001$; unpaired Mann–Whitney U-test.

F, G   Relative mRNA levels of endogenous *Calm3* transcripts (total and intron-retained isoform) upon exogenous TagRFP/TagRFP-Stau2 expression nucleofected rat cortical neurons DIV1 (F). The total Stau2 mRNA levels in these cells are also shown (G); $n = 3$. Bars represent mRNA levels mean + SEM normalized to control *PP1a* mRNA levels; t-test; *$P < 0.05$.

H   Relative mRNA levels of intron-retained GFP-$Calm3_L$ and GFP-$Calm3_{INT}$ transcripts to total *GFP* mRNA; graph represents mean ± SEM values normalized to respective controls, $n = 3$, t-test; $P > 0.05$.
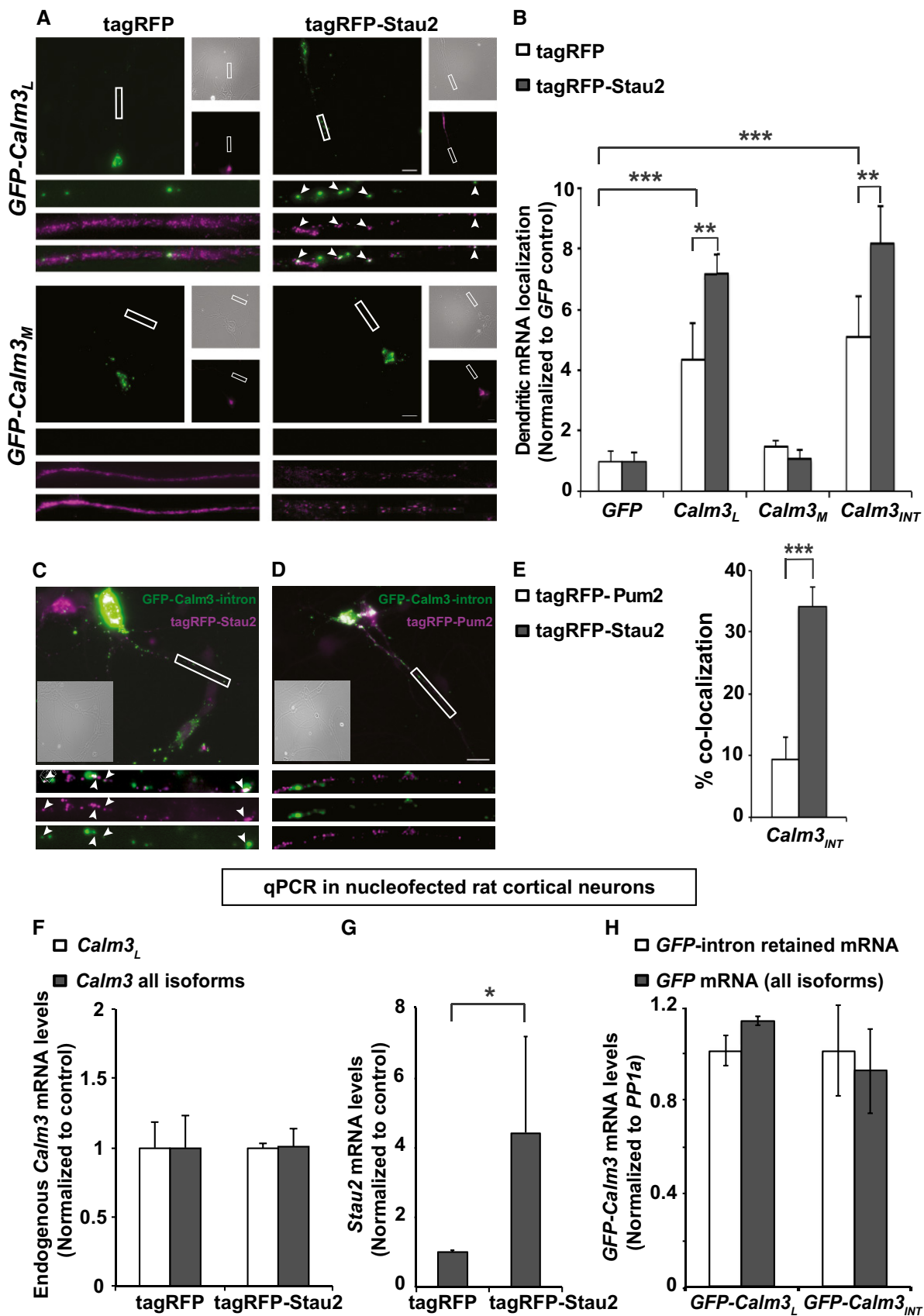
Figure 3.

Figure 4.

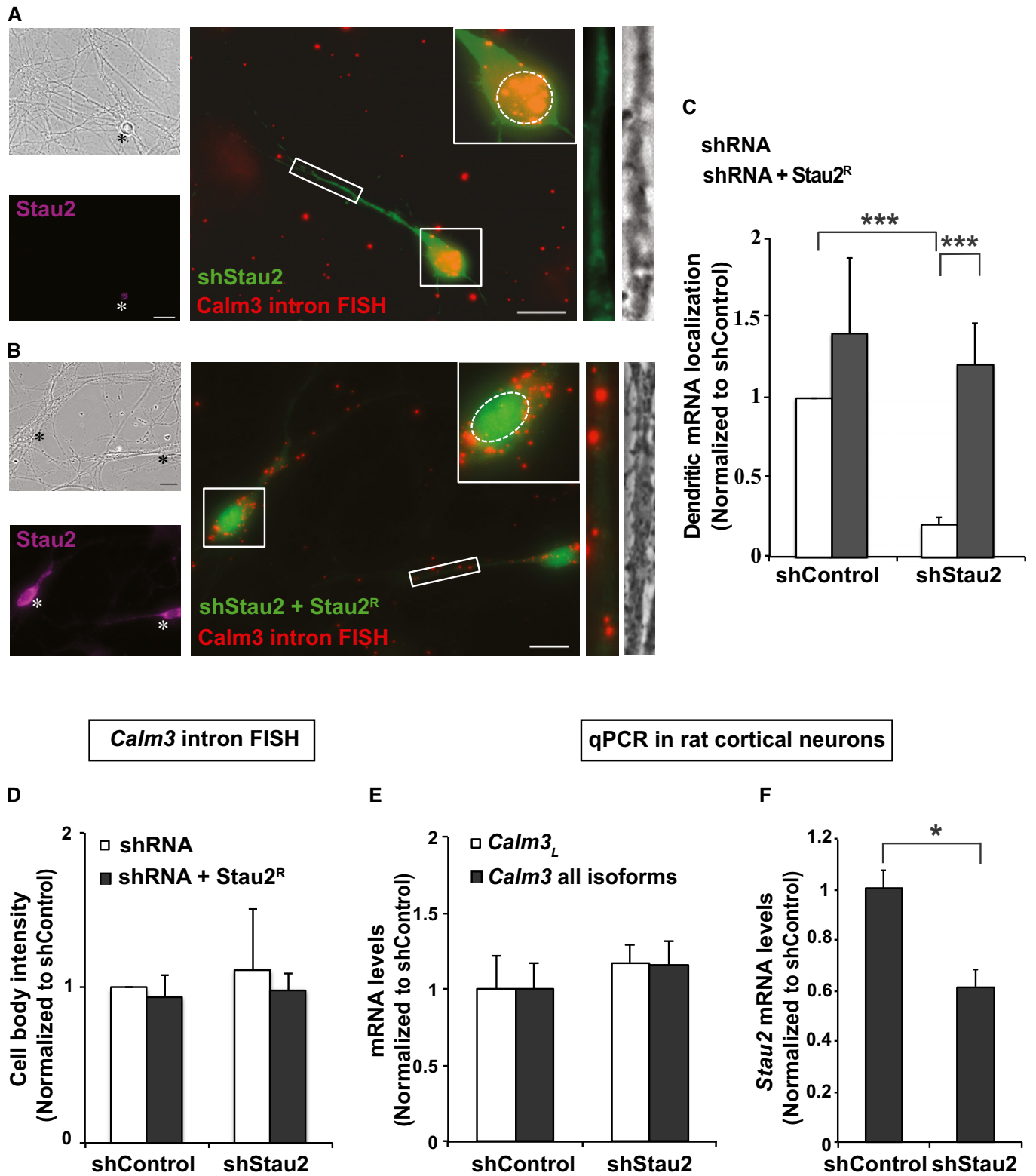*GFP-Calm3*$_{INT}$ transcripts co-localized with TagRFP-Stau2[62] as well (Fig 3C and E). This co-localization was specific for the *trans*-factor Stau2 since *GFP-Calm3*$_{INT}$ transcripts did not co-localize with

another RBP such as TagRFP-Pum2 (Fig 3D and E; *Calm3* mRNA does not harbor any consensus sites for Pum2 binding). Control experiments showed that Pum2 does not alter either the *Calm3*$_L$ or

Figure 4.   Dendritic localization of endogenous intron-containing *Calm3*$_L$ mRNA is regulated by Stau2 expression levels.

A   Representative image of cellular localization of endogenous *Calm3*$_L$ mRNA (identified by intron FISH) in a rat hippocampal neuron transfected with an shRNA to downregulate Stau2 (shStau2; green). Asterisks indicate Stau2 downregulated neurons (Stau2 levels were assessed by anti-Stau2 antibody staining; purple). Bright field is also shown. Magnified inset (soma) shows a relative increase in nuclear localization. Magnified box on the right shows a decreased number of dendritic *Calm3*$_L$ puncta in a 40-μm dendritic section marked with a white box and the corresponding phase image. The white perforated line marks the position of the nucleus. Scale bar, 20 μm.

B   Representative image of cellular localization of endogenous *Calm3*$_L$ mRNA (identified by intron FISH) in a rat hippocampal neuron co-transfected with an shRNA to downregulate Stau2 (shStau2; green) and an RNAi-resistant Stau2 rescue construct (Stau2^R). Selected dendritic regions were at least 2 cell body diameters away from the soma. Magnified box on the right shows the dendritic *Calm3*$_L$ puncta in a 40-μm dendritic section marked with a white box and the corresponding phase image. Panel on the lower left shows Stau2 immunostaining (purple), and panel on the upper left displays the corresponding bright field. Magnified inset (top right corner) shows the soma. The white perforated line marks the position of the nucleus. Asterisk denotes the soma of the neuron under study. Scale bar, 20 μm.

C   Quantification of dendritic *Calm3*$_L$ mRNA localization (identified by intron FISH) in the dendrites of neurons as in the experiments shown in (A) and (B). Bars represent the mean number of spots per 40-μm-long dendritic region normalized to control + SEM taken from three independent experiments. $n \geq 30$ dendrites per condition, ***$P < 0.001$; unpaired Mann–Whitney U-test.

D   Quantification of fluorescent intensity signal in the cell body to measure total levels of *Calm3*$_L$ mRNA [detected by *Calm3* intron FISH experiments as represented in panel (A) and (B)]. Bars represent mean values + SEM, normalized to respective controls, $n = 3$ experiments; t-test; $P > 0.05$.

E, F   qPCR to measure endogenous levels of *Calm3* (E) or Stau2 (F) in rat cortical neurons, where Stau2 was downregulated using an shRNA. $n = 3$ experiments, mean + SEM, t-test, *$P < 0.05$.

Calm3$_{INT}$ reporter expression in luciferase expression assays (data not shown).

Endogenous Stau2 regulates dendritic localization of *Calm3*$_L$ mRNA

Staufen forms RNPs that mediate localization of its target mRNAs in the *Drosophila* oocyte [19,20]. The mammalian homolog Stau2 has been implicated in dendritic mRNA localization [6,8]; however, a precise mechanism and its specificity remains elusive. In order to investigate whether mammalian Stau2 directly regulates the dendritic localization of endogenous C*alm3*$_L$ mRNA, we performed FISH in neurons in culture. Here, we observed that downregulation of Stau2 using transiently transfected shRNA (shStau2) [21] in rat hippocampal neurons led to substantial reduction of dendritically localized intron-retaining *Calm3*$_L$ transcripts (Fig 4A and C), while a control shRNA (shControl) did not (Fig EV4A). Importantly, the reduction in dendritic localization of *Calm3*$_L$ mRNA was completely rescued when an RNAi-resistant Stau2 (Stau2^R) [6] was co-expressed together with shStau2 (Fig 4B and C). Co-expression of Stau2^R together with an shControl plasmid did not further increase the dendritic localization of *Calm3*$_L$ mRNA significantly (Fig EV4B). Interestingly, the localization of the *Calm3*$_L$ isoform was mainly restricted to the nucleus in the absence of Stau2 (Fig 4A, inset) and this effect could also be rescued by co-expression of Stau2^R (Fig 4B, inset). Importantly, the total levels of the *Calm3*$_L$ mRNA isoform did not change upon Stau2 downregulation in hippocampal (Fig 4D) or cortical neurons (Fig 4E and F). Stau2 can shuttle between the nucleus and the cytoplasm [22]. The nuclear restriction of the *Calm3*$_L$ mRNA in the absence of Stau2 further suggests a role for Stau2 in the nucleus. Whether this is linked to its role in dendrites needs further investigation.

In summary, these experiments showed that mammalian Stau2 regulates the dendritic localization of the intron-containing *Calm3*$_L$ isoform in primary neurons without affecting its stability.

Together, our study has several implications. Genome-wide expression of mRNA with longer 3′-UTRs increases during development in brain and muscle [23], and such isoforms have an increased probability of localizing to neural projections of hippocampal neurons [24]. This is in line with our findings that the long isoform of *Calm3* containing the retained intron in its 3′-UTR is preferentially expressed in mature hippocampal neurons. Furthermore, it is this 3′-UTR intron that enables Stau2 binding and mediates its dendritic localization. Since this dendritic *Calm3*$_L$ mRNA localization is regulated by NMDA receptor activation, it is tempting to speculate that *Calm3*$_L$ recruitment enables local protein synthesis at synapses. Importantly, Stau2 recruitment to the retained intron in the *Calm3*$_L$ mRNA suggests that Stau2 recognizes RNA structure as an element mediating specificity. While such specific recruitment is clear for RBPs that bind in an mRNA sequence-dependent manner (in line with our "*RNA signature*" hypothesis [2]), there has been limited evidence for dsRBPs, like Stau2. In addition, the regulation of dendritic mRNA localization of *Calm3*$_L$, without changes in mRNA stability or decay, indicates that Stau2 performs distinct functions on specific targets. Importantly, the binding of Stau2 to 3′-UTR introns in other 27 mRNA targets ensues an elegant mechanism wherein Stau2 recruitment can be achieved by selective intron retention. This would then render its function regulatable in specific cell types or during developmental stages. This mechanism of intron retention would be of general importance not just for Stau2 but also in the case of other RBPs.

Materials and Methods

Immunoprecipitations and RNA isolation

Stau2 RNP isolation and immunoprecipitation (IP) were performed in triplicate as described [10,25]. Pre-immune serum was used to perform control IPs. Total RNA was isolated using mirVana™ miRNA isolation kit according to the manufacturer's instructions (Applied Biosystems). RNA was eluted, ethanol-precipitated, and resuspended in nuclease-free H$_2$O and RNA concentration measured using a NanoDrop spectrophotometer (Thermo Scientific). For quantification of mRNA levels in nucleofected rat cortical neurons, we used the QIAshredder and RNeasy kit (Qiagen) for RNA isolation. On-column DNase (Qiagen) treatment was performed before proceeding to cDNA synthesis. All steps were performed according to the manufacturer's instructions. For Northern blot analysis, total RNA was isolated from DIV11 rat cortical neurons (RCN). For quantification of endogenous Stau2 and *Calm3* (*Calm3*$_L$ and *Calm3* all isoforms) mRNA levels from 0/2/4/6–7 DIV RCN or from

E17.5/adult rat cortex, the total RNA was obtained using TRIZOL reagent (Thermo Scientific, 15596018) according to the manufacturer's instructions.

cDNA synthesis and quantitative RT–PCR

cDNA was synthesized from 0.5 to 1 μg DNase-treated RNA using random primers and Superscript III™ reverse transcriptase (Invitrogen) according to the manufacturer's instructions. For IPs, 0.5 μg of input RNA, 0.5 μg of IP RNA, and an equal volume of pre-immune IP RNA were used as template. To detect *Calm1*, *Calm2*, and *Calm3* mRNAs, quantitative reverse transcriptase PCR (qRT–PCR) was performed using the SYBR Green Master Mix (Bio-Rad) according to the manufacturer's instructions. Primers were optimized to achieve 95–105% efficiency; qRT–PCR data were analyzed using the comparative $\Delta\Delta C_T$ method [26]. For cDNA synthesis using total RNA isolated from rat cortical neurons, 2 μg total RNA for each sample was treated with 1 unit of DNase I (Thermo Fisher Scientific) at 37°C for 30 min. DNase-treated RNA was split in two: 1 μg was used for cDNA synthesis and the rest 1 μg for minus reverse transcriptase (−RT) reactions. Superscript III (#18080093; Thermo Fisher Scientific) was used to perform cDNA synthesis according to the manufacturer's instructions. For detecting mRNA levels by qPCR, a homemade SYBR Green Mix [containing the following components at a final concentration of 1 M betaine (B0300; Sigma), 1× standard Taq buffer (NEB), 16 μM dNTPs (N0447S; NEB), BSA 20 μg/ml (B9000S; NEB), 0.6 U per reaction Hot-Start Taq DNA polymerase (M0495S; NEB), and 1 μl/ml of 1:100 SYBR Green (20010; Lumiprobe)] (in ddH$_2$O) was used. Forward and reverse primer pair mix was used 2 μl per reaction from the following stock concentrations: Renilla and firefly luciferase at 3 μM, GFP 5 μM, and Calm3 ORF Fwd/Rev 2.5 μM; Calm3 ORF Fwd/Calm3 intron Rev 4 μM, Stau2 5 μM, pp1a 3 μM, GFP Fwd/Calm3 intron Rev 4 μM, and Renilla luciferase Fwd/Calm3 intron Rev 4 μM. Five microliters of a 1:10 dilution of cDNA was added to total 15 μl reaction, in duplicate for each primer set. −RT and ddH$_2$O controls were used for each sample. qPCRs were performed in a LightCycler 96 system (Roche) and analyzed using the comparative $\Delta\Delta C_T$ method [27]. *PP1a* mRNA levels were used as internal control for normalization. Primer sets were rigorously validated on dilution series and optimized to achieve 95–105% efficiency before use.

Stau2 iCLIP and analysis

We performed Stau2 iCLIP from E18 (embryonic day 18) mouse brain samples using anti-Stau2 antibodies [25] or the pre-immune serum (PIS) as a control according to a protocol described previously [14] with the following modifications. At the RNase digestion step, 20 U of RNase I (Thermo Fisher Scientific, #AM2295) was added to 1 ml of brain lysate. At the IP step, 450 μl of lysate was incubated with 2 μg of anti-Stau2 antibody for 2 h at 4°C, followed by incubation for 1 h at 4°C on a rotation wheel with 100 μl of protein G beads (Dynabeads, Thermo Fisher Scientific, #10004D). Upon SDS–PAGE and transfer to nitrocellulose, the region corresponding to the molecular weight larger than Stau2 (> 60 kDa) was excised and RNA was extracted from the membrane.

High-throughput sequencing was done using 50 cycles on Illumina GAII. The sequence reads were processed using the iCount server (http://icount.biolab.si) as described before [14]. Briefly, sequence reads are mapped to the mouse genome (mm9/NCBI37) using Bowtie software [28] with the following parameters (-v 2 -m1 -a –best –strata) and the mapped reads were collapsed referring the unique molecular identifiers included in the reverse transcription primer. The genomic regions were annotated using Ensembl annotation (V.59). The significant crosslinking clusters (flanking region of 15 nt and FDR < 0.05) were identified by comparing them with randomized control [13,14,29]. The randomers were registered and the barcodes were removed before mapping the sequences to the genome sequence allowing two mismatches using Bowtie version 0.12.7 (command line: -v 2 -m 1 -a –best –strata). The nucleotide preceding the iCLIP cDNAs mapped by Bowtie was used to define the crosslink sites identified by truncated cDNAs. The method for the randomer evaluation, annotation of genomic segments, and identification of significantly clustered crosslinking events was performed with FDR 0.05 and a maximum spacing of 15 nt, as described earlier [13], such that the positions of crosslink sites were randomized within individual RNA regions (i.e., introns, CDS, and UTRs separately). The replicate iCLIP experiments for the same protein were grouped before performing the analyses. We used Gencode annotation to define the RNA regions and identify 3′-UTRs containing retained introns.

Calm3 mRNA 3′-UTR secondary structure prediction

The minimum free energy secondary structure of mouse *Calm3* mRNA long 3′-UTR (TROMER Transcriptome database id: MTR004019.7.453.0) was predicted using the RNAfold program with the default parameters [30].

Primary neuron cultures, transfections, and pharmacological treatments

Embryonic day 17 (E17) hippocampal neurons were isolated from embryos of timed pregnant Sprague Dawley rats (Charles River) as described [6] and transfected using a calcium phosphate protocol [31,32]. For NMDA-mediated neuronal stimulation, after 24 h of expression of transfected plasmids, hippocampal neurons were treated for 10 s with 100 μM NMDA in Ca^{2+}/Mg^{2+}-free PBS and then incubated in B27-NMEM medium containing 100 μM NMDA for 15 min. Cells were then rinsed with HBSS and fixed. For neuronal silencing, after 6 h of expression of plasmids, cells were washed once with HBSS and then incubated overnight at 37°C in NMEM-B27 medium containing 100 μM 6-cyano-7-nitroquinoxaline-2,3-dione (CNQX), 50 μM 2-amino-5-phosphonopentanoic acid (AP5), and 1 μM tetrodotoxin (TTX). Cells were then washed twice with HBSS and fixed. Mock-treated cells were used as controls for both treatments. Where indicated, dissociated primary cortical neurons were prepared from rat cortices remaining from hippocampal dissections [10]. Rat primary cortical neurons (E17) were transfected using Amaxa Nucleofection (Rat Neuron Nucleofector Kit, Lonza, program O-003 according to the manufacturer's instructions).

Imaging-based GFP expression assay in primary neurons

Gene fragments of interest were cloned downstream of the GFP gene into the pEGFP vector under the control of a shorter version of the synapsin promoter. As control, empty GFP reporter plasmid was used. DIV11 primary rat hippocampal neurons were co-transfected with 1.5 µg of reporter plasmid and 1.5 µg of TagRFP or TagRFP-Stau2 or TagRFP-Pum2 plasmid using calcium phosphate and fixed at DIV12 for performing FISH as described below.

FISH and immunocytochemistry

Fluorescence *in situ* hybridization using tyramide signal amplification was performed as described [33,34]. The following RNA probes were used: *Calm3* intron and *GFP* sense and antisense from a cloned pBluescript II KS$^+$ construct described below. Immunocytochemistry was performed as previously described [34]. For FISH following Stau2 knockdown, DIV11 primary hippocampal neurons were transfected (co-transfection of control/Stau2 shRNA with either TagRFP or RNAi-resistant TagRFP-Stau2 62-kDa isoform) using calcium phosphate and fixed at DIV16. For *GFP* mRNA FISH, DIV11 primary hippocampal neurons were transfected [co-transfection of GFP constructs containing different *Calm3* 3′-UTRs with either TagRFP or TagRFP-Stau2 (i.e., the 62-kDa isoform)] using calcium phosphate and fixed at DIV12.

Imaging and statistical data analysis

Images were acquired in Zen acquisition software using an Observer Z1 microscope (both from Zeiss) with a 63× planApo oil immersion objective (1.40 NA) and a CoolSnap HQ2 camera (Olympus). For FISH experiments, *z*-stacks of neurons were acquired (50 stacks with optimal step size suggested by the Zen acquisition software ~0.26 nm). Images were then deconvoluted using the Zen deconvolution module. For quantification, imaging and selection of 40-µm dendritic regions for each image was done. Images were then projected orthogonally. The *Analyze particles* plugin in the ImageJ software was used for quantifying the number of spots per 40-µm dendritic region that was at least 2 cell body diameters away from the soma. For cell body intensity quantification from FISH images, the *measure* function in the ImageJ software was used. The average intensity/µm^2 of each soma was quantified.

For quantifying co-localizing events between *GFP-Calm3$_{INT}$* and TagRFP-Stau2^{62}, a deconvoluted set of images were selected and manually scored by two independent observers. Percentage of total *GFP-Calm3$_{INT}$* particles (in a 100-µm dendritic region) co-localizing with TagRFP-Stau2^{62} were quantified. We used TagRFP-Pum2 as control in parallel. For quantifying co-localizing events, a deconvoluted set of *z*-stacks was selected and manually scored blind to the experimental conditions (without knowing whether it was TagRFP-Stau2 or TagRFP-Pum2) by two independent observers. Only the spots that were in the same plane and had their center of focus co-localizing were scored as co-localization events. Individual "blind" scores were then averaged, and the data were presented as percentage of total particles

co-localizing in a 40-µm dendrite (2 cell body diameters away from the soma).

For all experiments, ≥ 30 dendrites (1 dendrite per neuron)/ ≥ 30 cell body per set from three independent experiments were selected for quantification. The conditions of experiments were kept blind for the observer until final analysis. GraphPad Prism 7.0 software was used to test the normal distribution of the data (D'Agostino–Pearson omnibus test) and for significance testing before decision of the statistical test to be used. Normalized values were used to determine significant differences with the unpaired Mann–Whitney *U*-test for samples with unequal variances. All graphs were plotted in MS Excel.

Antibodies

Primary antibodies: Mouse monoclonal and rabbit polyclonal anti-Stau2 antibodies (both used at 1:500 dilution) [35] were generated by affinity purification from existing immune sera; polyclonal anti-GFP antibodies were a gift from Werner Sieghart (CBR, Vienna, Austria) (used at 1:5,000 dilution). The following commercial antibodies were used: rabbit polyclonal anti-RFP (1:4,000) (Life Technologies, R10367); and monoclonal anti-MAP2 (1:500) (Sigma-Aldrich, M4403).

Secondary antibodies: Donkey anti-mouse A488-, A555-, or A647-conjugated antibodies and donkey anti-rabbit A555- or A647-conjugated antibodies (all from Life Technologies) were used at 1:1,000 dilution.

Plasmids

shControl (Dharmacon) and shStau2 [21] sequences were cloned into the pSuperior + GFP vector system as described. Full-length *Calm3* 3′-UTR was PCR-amplified from a rat EST plasmid obtained from ImaGenes (IMAGp998L0619945Q) (accession number AF231407), using the primers Calm3$_L$ Fwd and Rev, and then cloned into the psiCHECK2 vector (Promega) as described [10]. For cloning the *Calm3* intron, the primers Calm3$_{INT}$ Fwd and Rev were used, and it was cloned into pEGFP-C2 vector via EcoRI/BamHI and then further sub-cloned into pBluescript KS$^+$ vector via SacI/BamHI (for FISH probes) and into psiCHECK2 (Promega) dual-luciferase reporter plasmid via SacI/SalI for qPCR on luciferase reporters.

Intermediate *Calm3* 3′-UTR (Calm3$_M$) was PCR-amplified from a rat EST plasmid obtained from ImaGenes (IRBQp994H052D) (accession number AF231407), using the primers Calm3$_M$ Fwd and Rev, and then cloned into psiCHECK2 plasmid via SalI/NotI. The CMV promoter in pEGFP-C1 plasmid was replaced by synapsin (Syn) short promoter using the following primers: Syn Fwd and Rev. This construct was then used to generate *GFP* constructs with *Calm3* full-length 3′-UTR (*GFP-Calm3$_L$*) via HindIII/SalI, *Calm3* intermediate 3′-UTR (*GFP-Calm3$_M$*) via HindIII/SalI, and *Calm3* intron (*Calm3$_{INT}$*) via EcoRI/BamHI. The coding sequence for 62-kDa isoform of Stau2 was cloned into pTagRFP vector using the following primers: Stau2 Fwd and Rev via XhoI/SacI. The RNAi-resistant Stau2 (Stau2^R) (in pEGFP-N1) generated previously [6] was sub-cloned into pTagRFP-C. See the "Primers and shRNA sequences" section below.

Northern blot

10–15 µg of total RNA from cortical neurons DIV11 was electrophoresed in agarose–formaldehyde gels (1%), transferred to Nytran membranes (Hybond-N, Amersham), hybridized following standard procedures [36], and analyzed using PhosphorImager screens in a Typhoon FLA9500 multi-mode imaging scanner and Fiji software. Fragments of open-reading frames (ORF) and 3′-UTR intron were obtained by PCR and cloned into pBluescript KS$^+$ plasmid (see primer sequences below). Double-stranded DNA was obtained afterward by restriction endonuclease digestion and radiolabelled using the random primer PrimeIt kit (Stratagene) and [α-^{32}P]dCTP.

Luciferase reporter mRNA expression and RNA isolation

Gene fragments of interest were cloned downstream of the Renilla luciferase (Luc) gene into the psiCHECK2 vector (Promega). As control, empty Luc reporter plasmid was used. HeLa cells (plated in 24-well plates with 100,000 cells per well) were transfected with 0.1 µg of reporter plasmid and 0.4 µg of TagRFP or TagRFP-Stau2 plasmid (per well) using Lipofectamine

Primers and shRNA sequences

Primer name	Species	Primer sequence (5′–3′)
(qPCR) Calm1	*Rattus norvegicus*	Fwd: TTCCCCCTCTAGAAGAATCAAA
		Rev: CCACCAACCAATACATGCAG
(qPCR) Calm2	*Rattus norvegicus*	Fwd: AAGGTTCCCCCACTGTCAGA
		Rev: AAGCCACATGCAACATGGTA
(qPCR) Calm3	*Rattus norvegicus*	Fwd: ACAGCGAGGAGGAGATACGA
		Rev: CATAATTGACCTGGCCGTCT
(qPCR) Firefly luciferase	*Photinus pyralis*	Fwd: GAGTCTATCCTGCTGCAGCAC
		Rev: CTCGTCCACGAACACCACTC
(qPCR) Renilla luciferase	*Renilla reniformis*	Fwd: GTCCGGCAAGAGCGGGAATGG
		Rev: ACGTCCACGACACTCTCAGCAT
(qPCR) Calm3$_L$	*Rattus norvegicus*	Calm3 ORF Fwd: GGAGACGGCCAGGTCAATTATGC
		Calm3 intron Rev: GTCACCCAAAAGAAGGGCAAACC
(qPCR) Pp1a	*Rattus norvegicus*	Fwd: GTCAACCCCACCGTGTTCTTG
		Rev: CTGCTGTCTTTGGAACTTTG
(qPCR) Stau2	*Rattus norvegicus*	Fwd: GAACATCTCCTGCTGCTGAAG
		Rev: ATCCTTGCTAAATATTCCAGTTGT
(qPCR) GFP	*Aequorea victoria*	Fwd: ACCCAGTCCGCCCCTGAGCAA
		Rev: GCGGCGGTCACGAACTCCAG
(Cloning) Calm3$_L$	*Rattus norvegicus*	Fwd: AGGCCCGGGCAGCT
		Rev: GGTAGTCACTGTATTTTATTGGAAAACA
(Cloning) Calm3$_{INT}$	*Rattus norvegicus*	Fwd: GAATTCGGGAGCCTCTGC
		Rev: CTGGGCAGGTCCCAGGGATCC
(Cloning) Calm3$_M$	*Rattus norvegicus*	Fwd: ACTTCAGTCGACAGGCCCGGGCAGCTGGC
		Rev: CTGGTTGCGGCCGCGGTAGTCACTGTATTTTATTGGAAAAC
(Cloning) Stau2^{62}	*Rattus norvegicus*	Fwd: ATGGCAAACCCCAAAGAGAA
		Rev: CTAGATGGCCGACTTTGATTTC
(Cloning) Syn	*Rattus norvegicus*	Fwd: ATACCCTGTGTCATTCCTTGTT
		Rev: GGTGGCAGCTTGGGGCA
Calm3 ORF (Northern blot)	*Rattus norvegicus*	Fwd: CATGGCTGACCAGCTGACC
		Rev: CACTTCGCAGTCATCATCTGTAC
Calm3 3′-UTR intron (Northern blot)	*Rattus norvegicus*	Fwd: GGTCTCACTGACGCGTGTTCT
		Rev: GGCAGAAAGCGATGCCAAGT
shStau2	*Rattus norvegicus*	GATATGAACCAACCTTCAA
shControl	*Rattus norvegicus*	GATCCCCCTCCAAAGTTCGATGGTTTTCAAGAGAAACCATCGAACTTTGGAG

2000 (Invitrogen). Total RNA was isolated 24 h after transfection. For quantification of luciferase mRNA levels in Lipofectamine-transfected HeLa cells, we used the QIAshredder and RNeasy kit (Qiagen) for RNA isolation. On-column DNase (Qiagen) treatment was performed before proceeding to cDNA synthesis. All steps were performed according to the manufacturer's instructions.

Data availability section

Primary data
Stau2-iCLIP data were submitted to ArrayExpress. It can be accessed through the following link: http://www.ebi.ac.uk/arrayexpress/experiments/E-MTAB-5703.

Referenced data
iCLIP data for the RBPs TDP-43 and FUS from E18 mouse brains are published [14]. The Stau2 IP data from E17 rat brains are published as well [10].

Expanded View for this article is available online.

Author contributions

JU and MAK conceived the project. TS, YS, JH-F, SMF-M, IRM, and JE conducted experiments. All authors analyzed data. TS and MAK wrote the manuscript with feedback from all coauthors. JU and MAK provided resources and supervision.

Conflict of interest

The authors declare that they have no conflict of interest.

References

1. Tanaka J, Horiike Y, Matsuzaki M, Miyazaki T, Ellis-Davies GC, Kasai H (2008) Protein synthesis and neurotrophin-dependent structural plasticity of single dendritic spines. *Science* 319: 1683–1687

2. Doyle M, Kiebler MA (2011) Mechanisms of dendritic mRNA transport and its role in synaptic tagging. *EMBO J* 30: 3540–3552

3. Turrigiano G (2011) Too many cooks? Intrinsic and synaptic homeostatic mechanisms in cortical circuit refinement. *Annu Rev Neurosci* 34: 89–103

4. Norris AD, Calarco JA (2012) Emerging roles of alternative pre-mRNA splicing regulation in neuronal development and function. *Front Neurosci* 6: 122

5. Mayr C (2016) Evolution and biological roles of alternative 3′UTRs. *Trends Cell Biol* 26: 227–237

6. Goetze B, Tuebing F, Xie Y, Dorostkar MM, Thomas S, Pehl U, Boehm S, Macchi P, Kiebler MA (2006) The brain-specific double-stranded RNA-binding protein Staufen2 is required for dendritic spine morphogenesis. *J Cell Biol* 172: 221–231

7. Kusek G, Campbell M, Doyle F, Tenenbaum SA, Kiebler M, Temple S (2012) Asymmetric segregation of the double-stranded RNA binding protein Staufen2 during mammalian neural stem cell divisions promotes lineage progression. *Cell Stem Cell* 11: 505–516

8. Tang SJ, Meulemans D, Vazquez L, Colaco N, Schuman E, Hhmi C (2001) A role for a rat homolog of staufen in the transport of RNA to neuronal dendrites. *Neuron* 32: 463–475

9. Vessey JP, Amadei G, Burns SE, Kiebler MA, Kaplan DR, Miller FD (2012) An asymmetrically localized Staufen2-dependent RNA complex regulates maintenance of mammalian neural stem cells. *Cell Stem Cell* 11: 517–528

10. Heraud-Farlow JE, Sharangdhar T, Li X, Pfeifer P, Tauber S, Orozco D, Hörmann A, Thomas S, Bakosova A, Farlow AR *et al* (2013) Staufen2 regulates neuronal target RNAs. *Cell Rep* 5: 1511–1518

11. Laver JD, Li X, Ancevicius K, Westwood JT, Smibert CA, Morris QD, Lipshitz HD (2013) Genome-wide analysis of Staufen-associated mRNAs identifies secondary structures that confer target specificity. *Nucleic Acids Res* 41: 9438–9460

12. Ricci EP, Kucukural A, Cenik C, Mercier BC, Singh G, Heyer EE, Ashar-Patel A, Peng L, Moore MJ (2013) Staufen1 senses overall transcript secondary structure to regulate translation. *Nat Struct Mol Biol* 21: 26–35

13. König J, Zarnack K, Rot G, Curk T, Kayikci M, Zupan B, Turner DJ, Luscombe NM, Ule J (2011) iCLIP reveals the function of hnRNP particles in splicing at individual nucleotide resolution. *Nat Struct Mol Biol* 17: 909–915

14. Rogelj B, Easton L, Bogu GK, Stanton L, Rot G, Curk T, Zupan B, Sugimoto Y, Modic M, Haberman N *et al* (2012) Widespread binding of FUS along nascent RNA regulates alternative splicing in the brain. *Sci Rep* 2: 603

15. Palfi A, Kortvely E, Fekete E, Kovacs B, Varszegi S, Gulya K (2002) Differential calmodulin gene expression in the rodent brain. *Life Sci* 70: 2829–2855

16. Sugimoto Y, Vigilante A, Darbo E, Zirra A, Ambrogio AD, Luscombe NM, Ule J (2015) hiCLIP reveals the *in vivo* atlas of mRNA secondary structures recognized by Staufen 1. *Nature* 519: 491–494

17. Dotti CG, Banker G (1987) Experimentally induced alteration in the polarity of developing neurons. *Nature* 330: 254–256

18. Hutten S, Sharangdhar T, Kiebler M (2014) Unmasking the messenger. *RNA Biol* 11: 992–997

19. Ferrandon D, Elphick L, Nüsslein-Volhard C, St Johnston D (1994) Staufen protein associates with the 3′UTR of bicoid mRNA to form particles that move in a microtubule-dependent manner. *Cell* 79: 1221–1232

20. St Johnston D, Beuchle D, Nüsslein-Volhard C (1991) Staufen, a gene required to localize maternal RNAs in the *Drosophila* egg. *Cell* 66: 51–63

21. Mikl M, Vendra G, Kiebler MA (2011) Independent localization of MAP2, CaMKIIα and β-actin RNAs in low copy numbers. *EMBO Rep* 12: 1077–1084

22. Macchi P, Brownawell AM, Grunewald B, DesGroseillers L, Macara IG, Kiebler MA (2004) The brain-specific double-stranded RNA-binding protein Staufen2. Nucleolar accumulation and isoform-specific exportin-5-dependent export. *J Biol Chem* 279: 31440–31444

23. Ji Z, Lee J, Pan Z, Jiang B, Tian B (2009) Progressive lengthening of 3_ untranslated regions of mRNAs by alternative polyadenylation during mouse embryonic development. *Proc Natl Acad Sci USA* 106: 7028 – 7033

24. Taliaferro J, Vidaki M, Oliveira R, Olson S, Zhan L, Saxena T, Wang ET, Graveley BR, Gertler FB, Swanson MS *et al* (2016) Distal alternative last exons localize mRNAs to neural projections. *Mol Cell* 61: 821 – 833

25. Fritzsche R, Karra D, Bennett KL, Ang FY, Heraud-Farlow JE, Tolino M, Doyle M, Bauer KE, Thomas S, Planyavsky M *et al* (2013) Interactome of two diverse RNA granules links mRNA localization to translational repression in neurons. *Cell Rep* 5: 1749 – 1762

26. Livak KJ, Schmittgen TD (2001) Analysis of relative gene expression data using real-time quantitative PCR and the 2(-Delta Delta C(T)) Method. *Methods* 25: 402 – 408

27. Schmittgen TD, Livak KJ (2008) Analyzing real-time PCR data by the comparative C T method. *Nat Protoc* 3: 1101 – 1108

28. Langmead B, Trapnell C, Pop M, Salzberg S (2009) Ultrafast and memory-efficient alignment of short DNA sequences to the human genome. *Genome Biol* 10: R134

29. Wang Z, Kayikci M, Briese M, Zarnack K, Luscombe N, Rot G, Zupan B, Curk T, Ule J (2010) iCLIP predicts the dual splicing effects of TIA-RNA interactions. *PLoS Biol* 8: e1000530

30. Gruber A, Lorenz R, Bernhart S, Neuböck R, Hofacker I (2008) The Vienna RNA websuite. *Nucleic Acids Res* 36: W70 – W74

31. Dahm R, Zeitelhofer M, Götze B, Kiebler M, Macchi P (2008) Visualizing mRNA localization and protein synthesis in neurons. *Methods Cell Biol* 85: 293 – 327

32. Zeitelhofer M, Karra D, Vessey J, Jaskic E, Macchi P, Thomas S, Riefler J, Kiebler M, Dahm R (2007) High-efficiency transfection of mammalian neurons via nucleofection. *Nat Protoc* 2: 1692 – 1704

33. Heraud-Farlow JE, Sharangdhar T, Kiebler MA (2015) Fluorescent *in situ* hybridization in primary hippocampal neurons to detect localized mRNAs. In *In situ hybridization methods*, Hauptmann G (ed.), Neuro-methods, Vol. 99, Chapter 16, pp. 321 – 337. New York: Springer Science+Business Media

34. Vessey JP, Macchi P, Stein JM, Mikl M, Hawker KN, Vogelsang P, Wieczorek K, Vendra G, Riefler J, Tübing F *et al* (2008) A loss of function allele for murine Staufen1 leads to impairment of dendritic Staufen1-RNP delivery and dendritic spine morphogenesis. *Proc Natl Acad Sci USA* 105: 16374 – 16379

35. Zeitelhofer M, Karra D, Macchi P, Tolino M, Thomas S, Schwarz M, Kiebler M, Dahm R (2008) Dynamic interaction between P-bodies and transport ribonucleoprotein particles in dendrites of mature hippocampal neurons. *J Neurosci* 28: 7555 – 7562

36. Ausubel F, Brent R, Kingston RE, Moore DD, Seidman J, Smith JA, Struhl K (1997) *Short protocols in molecular Biology – A compendium of methods from current protocols in molecular biology*. New York: John Wiley & Sons